Methyl Group Dynamics in Glassy Polyisoprene: A Neutron Backscattering Investigation

B. Frick*

Institut Laue Langevin, BP 156X, F-38042 Grenoble, France

L. J. Fetters

Exxon Research and Engineering Company, Corporate Research Laboratories, Annandale, New Jersey 08801

Received September 1, 1993; Revised Manuscript Received November 22, 1993®

ABSTRACT: Energy-resolved, elastic neutron backscattering was employed to investigate the methyl group dynamics in polyisoprene between $T = 2$ K and room temperature. The use of partially deuterated samples (PI-d_5, PI-d_3, and PI-d_8) and of a fully protonated sample (PI-h_8) allowed the separation of the dynamics arising from the methyl group and from the backbone. A two-step relaxation is observed and attributed to the methyl group rotation at low temperatures and to the main-chain relaxation close to the glass transition. An Arrhenius-like increase of the methyl group rotational correlation time $\tau = \tau_0 \exp(E_{act}/kT)$, with $E_{act}/k = 1550$ K ~ 12 kJ/mol and $\Gamma_0 \sim 1/\tau_0 = 23.5$ meV ($\tau_0 \sim 1.76 \times 10^{-13}$ s) describes well the midposition of the first elastic intensity decrease but not its breadth. A 3-fold jump model with a broad Gaussian distribution of activation energies ($dE/E \sim 25\%$) around 1500 K can account for the observed temperature decrease. Inconstancies in the Q-dependence might be due to disorder effects. The torsional mode of the methyl group rotation is directly observed at $\Gamma_0 = 23.5$ meV by time-of-flight. Near the glass transition temperature a further decrease of the elastic scattering is observed due to the onset of a fast dynamics of the backbone in the picosecond range.

Introduction

Methyl group rotations and tunneling phenomena of methyl groups have been studied in some detail on low molecular weight materials. For polymers there is much less information on the dynamics of methyl groups. Initial neutron scattering studies with respect to the dynamics of methyl groups have been carried out on several polymers (e.g., refs 1–5), and the fixed-window technique reported here was applied to PDMS.[5] We have recently applied the same technique to study the dynamics of polymers near the glass transition for the related polymer 1,4-polybutadiene.[6,7] We could show that a fast dynamic process sets in near the glass transition temperature T_g. A comparison of the dynamic structure factors of polybutadiene and polysioprene had already given indications for methyl group rotations,[8] but the use of fully protonated polyisoprene in this study did not allow a separation of the different dynamic processes. Here we report a temperature-dependent study of the dynamics of the methyl groups on partially deuterated polyisoprenes over a wide temperature range, applying the neutron fixed energy window technique, which is described shortly. We summarize some theoretical considerations for methyl group rotations and incoherent neutron scattering before we present and discuss the experimental results.

Fixed-Window Technique and Incoherent Scattering

The incoherent scattering law $S_M^{inc}(Q,\omega)$ for scatterers undergoing reorientational motions within a certain volume may be written as[9]

$$S_M^{inc}(Q,\omega) \approx f_0(Q)\,\delta(\omega) + \sum_{i=1}^{n} f_i(Q)\,L_i(Q,\omega,\Gamma_i) \qquad (1)$$

with $\delta(\omega)$ being the delta function and $L_i(Q,\omega,\Gamma_i)$ normalized Lorentzian functions. Thus for a motion confined within a certain volume, the scattering function can be separated into an elastic and a quasielastic part, $f_i(Q)$ being the elastic and inelastic structure factors, for which a sum rule holds:

$$\sum_{i=0}^{n} f_i(Q) = 1 \qquad (2)$$

Let us consider in more detail two examples which will be relevant for this paper (for further information, see, e.g., ref 9). In the case of methyl groups the scattering atoms may jump within a 3-fold potential (usually of the form $V(\phi) = {}^1/_2V_3[1 - \cos(3\phi)]$, where ϕ is the torsion angle) on a circle of radius R and the incoherent scattering can in the powder case be written as in eq 1, with[9]

$$f_0(Q) = {}^1/_3[1 + 2j_0(3^{1/2}QR)]$$

$$f_1(Q) = f_2(Q) = {}^1/_3[1 - j_0(3^{1/2}QR)] \qquad (3)$$

$$\Gamma_i \sim \frac{1}{\tau_i} = \frac{1.5}{\tau}$$

where j_0 is the spherical Bessel function, and τ_i is the average residence time between two jumps.

We also note the case for isotropic rotational diffusion on a sphere with radius R:

$$f_0(Q) = j_0^2(QR) \qquad \tau_i^{-1} = i(i+1)D_R \qquad (4)$$

$$f_i(Q) = (2i+1)j_i^2(QR) \qquad i = 1,\infty$$

with D_R being the rotational diffusion constant and $j_i(QR)$ the Bessel function of the order i. In fact, for modeling we are using a recursion formula for eq 4 up to the order of $i = 9$.

Due to vibrations of the scatterers the scattering law in eq 1 must be multiplied by a Debye–Waller factor (DWF), which weakens both the elastic and inelastic parts of the scattering function. The inelastic scattering from phonons is usually assumed to be well separated and located at

® Abstract published in *Advance ACS Abstracts*, January 15, 1994.

0024-9297/94/2227-0974$04.50/0

higher energy. We also include an elastic fraction $c_{fix} < 1$ to take account of scatterers which do not participate in a certain type of reorientational motion, e.g., in our case the backbone atoms, which do not undergo 3-fold rotations like the methyl group protons. Nevertheless the scattering from these atoms will be weakened by the DWF in the same way:

$$S^{inc}(Q,\omega) = e^{-Q^2\langle u^2\rangle/3}[(1 - c_{fix})S_M^{inc}(Q,\omega) + c_{fix}] \quad (5)$$

The above equations are dependent on temperature via the line width of the Lorentzian functions and the increase of $\langle u^2\rangle$ with temperature. Usually the quasielastic spectral functions $L_i(\omega)$ broaden with increasing temperature, depending on the activation energy E_{act} and the attempt frequency Γ_0 of the scattering atom, assuming, e.g., an Arrhenius behavior:

$$\Gamma(T) = \Gamma_0 \exp(-E_{act}/kT) \quad (6)$$

In a fixed elastic window scan, which we discuss here, we measure only the elastic part of the model scattering function eq 1. Thus for the observed intensity $I_{el}(Q,T,\omega=0)$, if we convolute with the instrumental resolution function $R(\omega)$, it holds that

$$I_{el}(Q,T,\omega\sim 0) = \int_{-\infty}^{\infty} S^{inc}(Q,\omega')\, R(\omega-\omega')\, d\omega'|_{\omega=0} \quad (7)$$

In the low-temperature limit, as long as the line widths are small with respect to the width of the instrumental resolution function $R(\omega)$, the total elastic and quasielastic intensity is measured. Thus, due to the sum rule eq 2, the observed intensity equals unity, besides sample- and probe-specific factors and the zero-point motion.

$$S_M^{inc}(Q,\omega) \approx \sum_{i=0}^{n} f_i(Q)\, \delta_i(\omega) = 1 \quad (8)$$

At higher temperatures, along with the strictly elastic scattering, the central part of the spectral functions $L_i(\omega)$ (see eq 1) will contribute to the observed intensity. However, in the high-temperature limit, the quasielastic line widths broaden and then these contributions will be negligible. Hence, we observe in good approximation the elastic incoherent scattering factor (EISF):

$$S_M^{inc}(Q,\omega) = f_0(Q)\, \delta(\omega) = f_0(Q) \quad \text{for } \Gamma_i \gg \text{resolution width} \quad (9)$$

As the EISF shows characteristic modulations in Q, depending on the geometry and type of motion of the scatterer, this can be a sensitive probe for the local dynamics. The study of the observed elstic intensity as a function of temperature yields, furthermore, information on activation energies and thus on the local potentials. To do this the observed fixed-window scans have to be compared to models like eqs 3 and 4 to account for the contributions of the central parts of the spectral functions $L_i(\omega)$. Unfortunately, if the vibrational or librational amplitudes are big enough, the characteristic Q-dependences of the EISF will be smeared out by the Debye–Waller factor (eq 5) and a discrimination between different models becomes difficult. Also only a part of the scatterers might produce the characteristic structure in Q, and in the worst case other scatterers might even undergo different types of motions, leading to a different behavior in Q.

In Figure 1 calculations for the fixed-window scans of two different types of models are shown as a function of Q^2 and temperature, assuming the Q and temperature range of the IN13 experiment on PI-h_8. This is shown for

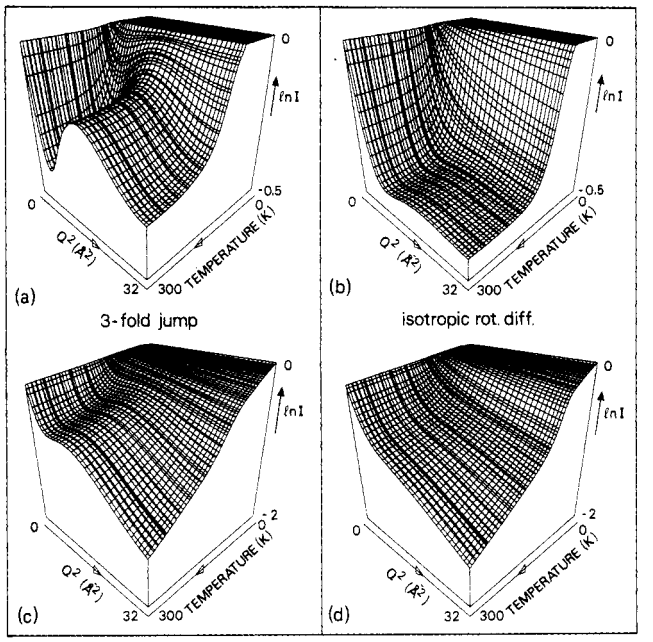

Figure 1. Model calculations for the elastic scattering of methyl protons as it should be observed as a function of Q^2 and temperature on IN3 (see text) applying (a) a 3-fold rotational jump model and (b) an isotropic rotational diffusion model. For short relaxation times with respect to the instrumental energy resolution, the elastic scattering resembles the elastic incoherent structure factor. Parts c and d correspond to parts a and b, respectively, but take an additional Debye–Waller factor into account, which smears the characteristic Q-dependences.

the case of an isotropic rotational model and for the case of a 3-fold jump model on a circle, both without (Figure 1a,b) and with influence of the Debye–Waller factor (Figure 1c,d).

The scattering function $S_M(Q,\omega)$ is proportional to the observed neutron intensity, with proportionality factors like the scattering cross sections (e.g., σ_{inc}(hydrogen) = 81 barn and σ_{inc}(deuterium) = 2.2 barn), the number of scattering atoms, and the incident and outgoing wave vectors of the neutron. These factors, however, will cancel if we normalize our data to another temperature run, preferably to a very low temperature, where the dynamics of the system is frozen and eq 8 holds.

The above equations are strictly valid for incoherent scattering. Coherent scattering can produce a static structure factor contribution which cancels due to the normalization only if negligible thermal expansion is present. This renders the discussion of Q-dependences difficult in the case of deuterated polyisoprenes. We summarize the coherent and incoherent scattering cross sections of the monomers and the methyl groups in Table 1.

For an exact consideration of the problem we also would have to take into account that multiple scattering is always present and changes with temperature. We deal with this contribution in approximate way: the multiple scattering contributions are visible through a temperature-dependent fraction for $Q \to 0$ in an $\ln(I)$ versus Q^2 plot which does not extrapolate to zero. In our modeling we will take this temperature-dependent but Q-independent contribution into account.

Samples

Partially deuterated polyisoprene samples were prepared in cyclohexane at 20 °C using *tert*-butyllithium as the initiator. The isoprene monomers were obtained from Cambridge Isotopes. Molecular weights (via size exclusion chromatography) ranged

Table 1. Neutron Scattering Cross Sections for Partially Deuterated Polyisoprene[a]

monomer	main chain coh	main chain inc	main chain tot	methyl group coh	methyl group inc	methyl group tot	%	total monomer
$CH_2CH{=}C(CH_3)CH_2$	36.6	399.5	436.1	5.28	239.7	244.98	35	681.1
$CD_2CD{=}C(CD_3)CD_2$	55.76	10.2	65.96	16.79	6.12	22.91	6.9	88.9
$CH_2CH{=}C(CD_3)CH_2$	36.6	399.5	436.1	16.79	6.12	22.91	1.3	459.0
$CD_2CD{=}C(CH_3)CD_2$	55.76	10.2	65.96	5.28	239.7	244.98	77	310.9

[a] In barns ($=10^{-28}$ m^2) (after ref 19). The scattering cross sections are given separately for the polymer backbone and the methyl side group (the methyl carbon is counted with the backbone). Coherent (coh), incoherent (inc), and total (tot) cross sections as well as the relative contribution of the methyl protons (deuterons) with respect to the total scattering from a monomer (%) are listed.

from 6.5×10^4 to 1.1×10^5. Heterogeneity indices, M_z/M_w and M_w/M_n, were 1.06 or less. The microstructure of the polyisoprenes was found to be via ^{1}H-NMR and ^{2}H-NMR ca. 93% 1,4-polyisoprene and 7% 3,4-polyisoprene.

The samples were squeezed to films of thicknesses between 0.2 and 1 mm, respectively, to get a transmission of roughly 85–90% and were kept in flat aluminum sample holders. In Table 1 we summarize the scattering cross sections for the differently deuterated polyisoprenes, separated into contributions from the backbone and the methyl group.

Instrumental Technique

Incoherent, energy-resolved elastic neuron scattering was carried out, applying the fixed-window technique. Thereby the neutron backscattering spectrometers IN10 and IN13 at the Institut Laue Langevin (ILL), Grenoble have been used, where an energy resolution of the order of 10^{-4} is achieved by monochromatizing and analyzing the incoming and scattered neutrons, respectively, close to a Bragg angle of 90°.[10] Whereas real spectroscopy can be carried out by putting the wavelength on the monochromator side out of tune against the analyzer side, in the fixed energy window technique, both analyzer and monochromator are held at the same wavelength, but the sample temperature is continuously varied. The instrumental energy resolution (fwhm) corresponds to 1 μeV, i.e., 4×10^{-9} s, at IN10, and to 8 μeV, i.e., 5×10^{-10} s, at IN13. Thus the dynamics of scattering particles being slower than a characteristic time corresponding to the energy resolution is seen as an elastic scatterer, whereas a decrease of the elastic intensity is observed for scattering on sample atoms which move faster. This not only allows the detection of the onset of fast motions but also gives insight into the geometry of motion via the intensity dependence on the momentum transfer $Q = 4\pi \sin(\theta)/\lambda$ (scattering angle = 2θ). The accessible Q-regimes are 0.2–2.2 Å^{-1} at IN10 and 0.6–5.2 Å^{-1} at IN13. The librational mode for the methyl group was measured at the time-of-flight instrument IN6 at the ILL with $\lambda_i = 5.1$ Å in energy gain.

Results and Discussion

We report first on fixed-window data taken on IN10 ($0.2 < Q < 2$ Å^{-1}) for hydrogenous polyisoprene (PI-h_8) and those with varying deuteration levels: PI-d_8, PI-d_5, and PI-d_3. The investigated temperature range covered in all these experiments was 2–300 K. The elastic scans for these polyisoprenes are shown for $Q \sim 1.95$ Å^{-1} in Figure 2. Clearly, a pronounced difference in the temperature dependence of the elastic scattering is observed for the differently labeled polymers. Whereas all the samples show a strong decrease of the elastic scattering near the calorimetric glass transition temperature (T_g = 215 K), a first steplike intensity decrease is observed only for samples for which the methyl group is protonated. We take this as a proof that the dynamics of the methyl group (first steplike decrease) can be separated from the dynamics of the backbone (second intensity decrease around T_g). More challenging is the determination of the exact type of motion which leads to the intensity decrease. In the following the dynamics at temperatures below $T = T_g$

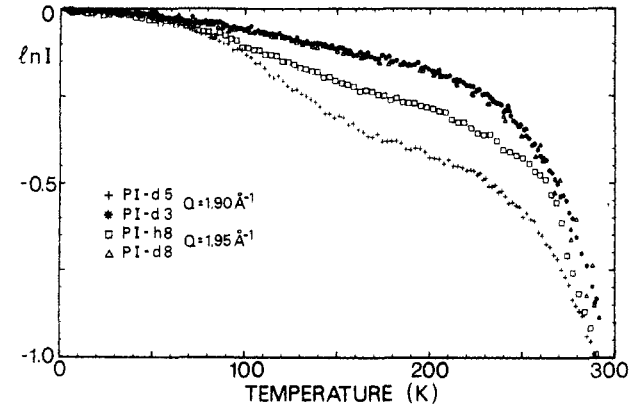

Figure 2. Elastic scattering as a function of temperature as observed on IN10 for differently deuterated polyisoprenes. The first relaxation step corresponds to the rotational dynamics of the methyl groups, and the second step corresponds to the onset of a fast dynamic process near the glass transition.

is discussed. A priori the following strategy seems to be reasonable: determination of the Debye–Waller factor on the sample where the backbone is protonated and where the methyl group to a first approximation does not contribute. Then, assuming that the DWF is the same for all four samples, model calculations could be done for the PI-d_5 sample, for which the scattering from the methyl group is enhanced. Taking into account that only a fraction of atoms take part in the reorientational motion, we might describe the intensity loss below the glass transition. The determination of the Debye–Waller factor must be done over a quite large Q-range to avoid mixing of contributions from the form factor of reorientational motions, which can give rise to a strong intensity decrease in the low Q-range (see Figure 1). Unfortunately, we have measurements over a wide Q-range only for PI-h_8. Therefore we tried to get the DWF for the different samples in agreement.

In Figure 3 we present the elastic scattering $\ln [I_{el}(Q,T)]$ of PI-h_8 plotted against temperature and Q^2 and normalized to $T = 2$ K as measured on IN13. The Q-range extends to 5.2 Å^{-1}, but data above $Q^2 \sim 20$ Å^{-2} are spoiled by Bragg intensities arising from the aluminum container and which appear from behind the shielding with increasing temperature. The sample temperature was scanned from T = 2 K to room temperature with a rate of 0.2 K/min, the intensities being updated every 10 min. The first observation one makes from these experimental data is the absence of a pronounced structure in Q (compare, e.g., Figure 1a). At the high-temperature and high-Q end the intensity falls considerably due to the strong increase of the mean squared displacement near the glass transition.[6,7] The absence of a clear struture in Q might well be a consequence of the Debye–Waller factor and that only a fraction of protons participates in the methyl group rotation. A comparison with Figure 1b,c where both terms are taken into account suggests that isotropic rotational

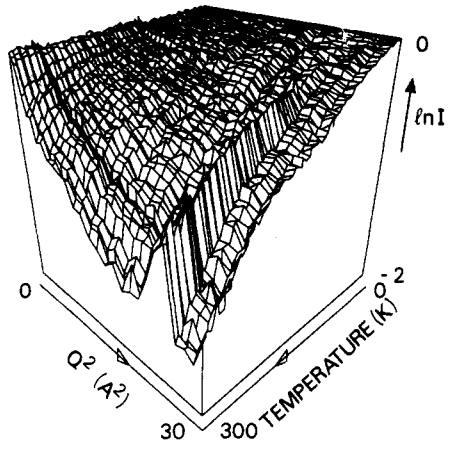

Figure 3. Elastic scattering of PI-h_8 as observed as a function of Q^2 and temperature on IN13 (the sharp peaks at high Q are due to contamination by the container Bragg peaks.

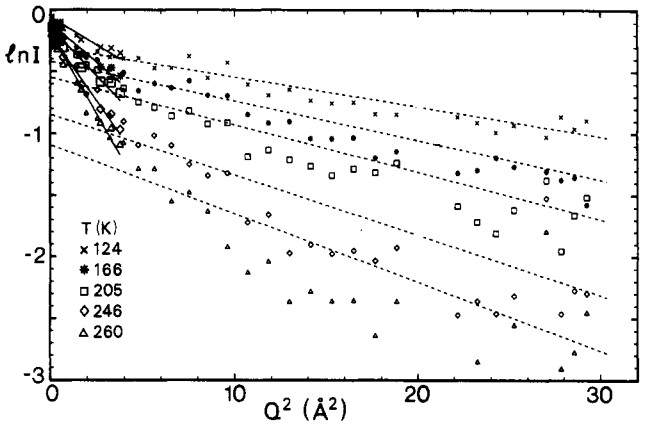

Figure 4. Logarithm of the elastic scattering on PI-h_8 as observed as a function of Q^2 at several temperatures on IN13. Clearly, a form factor deviating from a harmonic DWF can be observed.

diffusion, rather than a clear 3-fold jump on a circle, might be the model of choice.

To dwell more on the Q-dependence, we combine measurements on PI-h_8 in the low Q-range (from IN10 and IN13) and in the high Q-range (IN13). We plot in Figure 4 the logarithm of the elastic intensity normalized to the lowest temperature against Q^2 for several temperatures. In this presentation a straight line is expected for a Debye–Waller factor decrease of the intensity. For higher temperatures and at low Q-values the data fall off steeper than for the high Q-values. Two different Debye–Waller factors could be used to fit the data; a justification for such a procedure is, however, not evident. We conclude rather from modeling different situations that the steep decrease at low Q arises from a reorientational motion of protons and most probably from isotropic reorientation of the methyl group protons on a sphere of radius R = 1.027 Å. The lines indicate fits for straight lines for IN10 (solid lines and large symbols) and IN13 (dashed lines and small symbols), respectively. It is clearly seen that the IN10 data mainly mirror the form factor decrease and that the mean squared displacements extracted from this low Q-range are quite large.

From the Q-dependence we can deduce a reasonable value for the DWF by comparing the calculated, scattering amplitude weighted, effective mean squared displacements (msd) $\langle u^2 \rangle$ as a function of temperature and for the differently labeled PI samples (Figure 5). We call $\langle u^2 \rangle$ an effective msd because it includes contributions from main-chain oscillations as well as angular oscillations $\langle \phi^2 \rangle$, e.g., of the methyl protons. These contributions are weighted

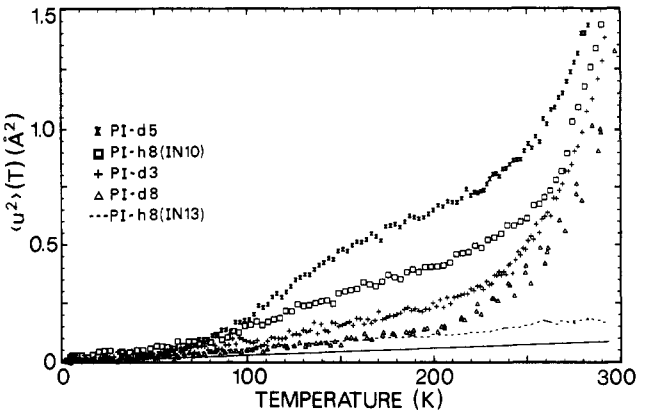

Figure 5. Effective, scattering amplitude weighted, mean squared displacement as a function of temperature as deduced from the elastic scattering at IN10 (symbols) and IN13 (dashed line). The solid line is the mean squared displacement which is attributed to the main-chain dynamics and which was used for the model calculations. The first low-temperature increase of the curves is due to the angular oscillations of the methyl group protons, and the second one is due to the onset of fast dynamics near the glass transition, which affects the main chain.

differently depending on the kind of deuteration. The msd for methyl protons only can be converted into angular oscillations $\langle \phi^2 \rangle$ by $\langle u^2 \rangle \sim 4R^2\langle \sin^2(\phi/2) \rangle$, with R = 1.027 Å. In Figure 5 the onset of the methyl group dynamics can be recognized for the protonated side group polymers. We deduce from this figure that the temperature range for which the mean squared displacement depends linearly on temperature, i.e., where $\langle u^2(T) \rangle = (\langle u^2(2\text{ K}) \rangle - \langle u_0^2 \rangle) + (\mathrm{d}\langle u^2 \rangle/\mathrm{d}T)T$, is quite narrow and we choose a value for $\mathrm{d}\langle u^2 \rangle/\mathrm{d}T$ which is compatible with all samples studied: The value $\mathrm{d}\langle u^2 \rangle/\mathrm{d}T = (2.9 \pm 0.1) \times 10^{-4}$ Å²/K was determined between 2 and 30 K and was used in the following models. This value corresponds to the msd of the main chain.

We also can get a rough estimate for the value of the msd at which the methyl group protons should start to move to the neighboring potential minima by applying the Lindeman criterion.[11] This should happen for $\langle u^2 \rangle \sim 0.1d$, where $d \sim 1.78$ Å is the distance between the potential minima, and thus we expect a stronger increase of transitions for $\langle \phi \rangle \gg \sim 12°$, i.e., for $\langle u^2 \rangle > \sim 0.185$ Å². Taking the uncertainty for the zero-point motion into account, we can see from Figure 5 that this value is reached for ca. 50–100 K in PI-d_5 in the range where the effective msd starts to deviate from the linear low-temperature (main chain) behavior.

Another plausible argument leads to an estimation of the opposite extreme, i.e., of the maximal displacement. Take again PI-d_5 for which mainly methyl protons, undergoing angular oscillations within the 3-fold potential, contribute to the observed msd. The protons will pass the potential well at the latest if the angular displacements reach a value of $d/2 \sim 0.89$ Å, i.e., half the distance between the potential minima. In Figure 5 we can see that an extrapolation of the msd for PI-d_5 would come close to this value if the sample would not pass the glass transition.

The ultimate aim is to describe the temperature decrease of the elastic scattering applying a plausible model for methyl group rotation. In Figure 6a we present the elastic scattering of PI-d_5 at Q = 1.97 Å^{-1}, the sample for which the observed scattering stems mainly from the methyl group protons. A two-step relaxation is clearly observed (MR rotation and structural relaxation). In Figure 6a we compare model calculations for the MR rotation with Γ_0 = 23.5 meV and an activation energy of 1400 K with the

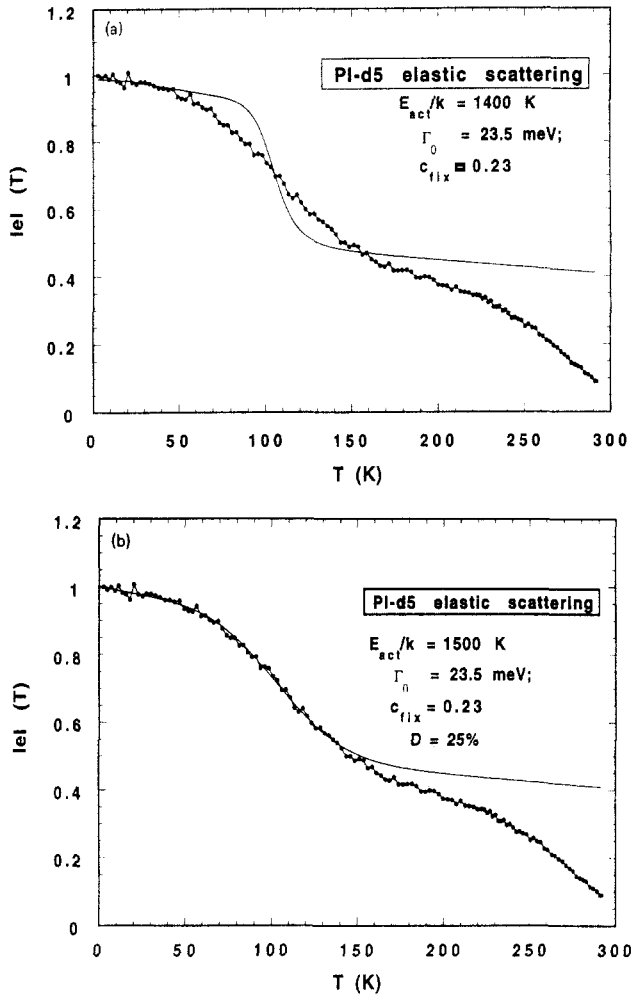

Figure 6. Model calculation for the first relaxation step of the methyl group rotation. The elastic part of the scattering law is calculated, assuming (a) E_{act} = 1550 K and Γ_0 = 23.5 meV for the methyl groups and a DWF for all protons and (b) the same parameters, but in addition a Gaussian distribution of activation energies around 23.5 meV.

experiment, weighted by the scattering strength of the methyl group protons and assuming that the elastic scattering from the polymer backbone decreases only via the DWF (eq 5). The frequency Γ_0 is taken from the librational mode position as observed in the measured vibrational density of states (see below). For all Q-values the above-mentioned parameters give a correct description of the midposition of the intensity drop, but the calculated drop is obviously much too sharp. An uncertainty in the instrumental energy resolution, which was assumed to be of Lorentzian shape with a 1-μeV fwhm, would not broaden the curve but only shift its midposition slightly.

To get a better agreement we have created a Gaussian distribution of activation energies on an energy grid of E_{act}/k = 25%, with otherwise the same parameters. As can be judged from Figure 6b we get a perfect agreement for the first relaxation step at Q = 1.97 Å^{-1}. We want to stress that the level to which the calculated curve relaxes was not adjusted but is merely a result of the assumed jump model for the methyl group protons and of the scattering strength with respect to the total monomer (c_{fix} in eq 5). The same parameters, however, describe the observed levels for the other six Q-values less well. As the radius of the circle on which the methyl protons move is quite precisely known—assuming that the backbone does not undergo large-amplitude motion—the Q-dependence of the high-temperature level should only be dependent on the choice of the model. On the other hand, neither rotational diffusion on a circle with R = 1.027 Å nor a 3-fold jump on the circle account correctly for the observed Q-dependence. At low Q-values the measured steplike decrease is too pronounced for all these models and could not even be explained by assuming c_{fix} = 0.

To get more information about the Q-dependence, we fitted the elastic scans for each Q-value with an elastic (c_{fix}) and a Lorentzian component only. The line with of the Lorentzian was assumed to broaden, Arrhenius like, with the best parameters for E_{act} and the distribution (activation energies around E_a = 1550 K with a width of 28 ± 4%). The fits result in a Q-dependence of the elastic fraction $c_{fix}(Q)$, from which we can estimate a jump distance. Comparing the EISF for rotational diffusion on a circle or 3-fold jump on a circle with radius R and subtracting the calculated c_{fix} from Table 1, we find that a radius $R \sim 1.027$ Å gives an average description of the remaining elastic component but that the experimental data are too low for $Q < 1$ Å$^-$ or too high for $Q > 1.2$ Å^{-1}.

Several explanations can be given for the inconsistent Q-behavior: (i) A distribution of activation energies, which has its origin in locally different environments, is an arbitrary choice to describe the disorder and may not properly account for the local heterogeneity, i.e., its Q-dependence. (ii) The calculated parameters c_{fix} in Table 1 result from the incoherent scattering strength with respect to the total scattering. The coherent contribution varies with Q and follows a static structure factor with a maximum around 1 Å^{-1} for PI-d_5; thus, c_{fix} may change slightly with Q. (iii) Multiple scattering introduces a stronger decrease with temperature at low Q-values (e.g., double scattering to twice a large angle) than calculated from the above models.

We should mention another possibility to explain the sluggish temperature decrease of the elastic intensity. If the high-temperature limit of the line width Γ_0 (see eq 6) is of the order of the instrumental energy resolution or somewhat smaller, then only the wings of the quasielastic scattering contributions will be lost from the measured elastic intensity. This also leads to a very slow intensity decrease with temperature. Assuming $\Gamma_0 \sim 0.4$ μeV ($\sim 10^{-8}$ s) and a low activation energy of $E_a/k \sim 270$ K (approximately the peak position of observed methyl libration), the fit to the experimental curve is not as good as for a distribution of activation energies but can roughly describe the slow decrease with temperature. The attempt frequency determined this way would be extremely low in comparison to other samples. In such a case the decrease of the elastic intensity would be a sensitive function of the exact shape of the resolution function, which was assumed to be perfectly Lorentzian. Thus we canot safely exclude these parameters in spite of a poorer fit.

We will compare our results with NMR T_1 measurements on polyisoprene.[13] The NMR experiment is selective for the methyl C–H vector reorientation and it was carried out at temperatures (300–400 K) much above T_g in contrast to our experiments. The rotation correlation time for the methyl group is given as (1–3) × 10^{-13} s for $T > 300$ K. The height of the potential was not specified, but it was suggested to be "substantially low". The correlation time deduced from this work agrees well with the high-temperature limit which we find, assuming an activation energy distribution (1.7×10^{-13} s). The authors also state that there is only a minor change of the correlation time between 300 and 400 K. Regarding that the methyl group protons due to our work have reached the high-temperature limit for the correlation time already at much lower temperatures, this is not astonishing. On the other hand,

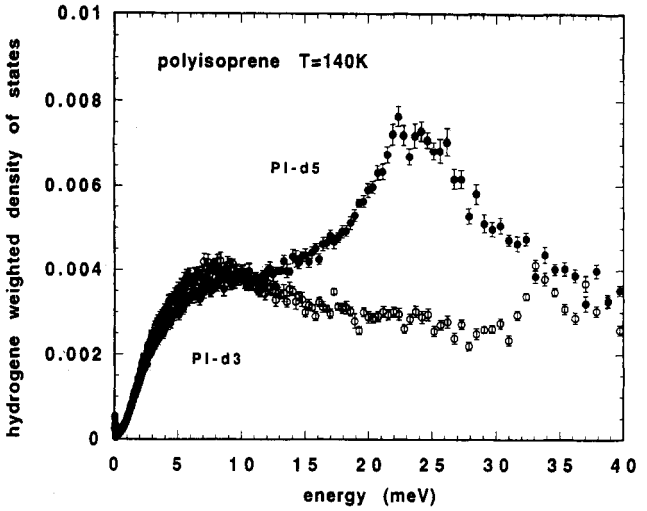

Figure 7. Hydrogen-weighted vibrational density of states at T = 140 K for differently deuterated polyisoprenes (measured in neutron energy gain on IN6, ILL, Grenoble). If the methyl group is protonated, the first librational transition is clearly observed at 23.5 meV. The broad contribution around 7 meV stems mainly from backbone oscillations.

the NMR result would not be consistent with the second set of parameters above ($\tau_0 \sim 10^{-8}$ s, $E_{act}/k \sim 270$ K); besides, one would assume a change of the activation behavior of the methyl groups at T_g.

In the following we report on the observation of the librational mode for methyl group rotation, which can be observed on neutron time-of-flight instruments. The hydrogen-weighted vibrational density of states was evaluated applying the incoherent Gaussian approximation and is shown for a neutron energy gain up to 40 meV for the PI-d_5 and the PI-d_3 sample (Figure 7). In both samples there appears a broad low-frequency hump around 7 meV, which arises from the diverse librational modes of the polymer backbone, and which is observed for polybutadiene, a main-chain polymer as well. Then, for PI-d_5 only, there appears a strong mode centered at 23.5 meV. (No angular dependence of the peak position is seen in the time-of-flight spectra.) We can be confident to assign this mode to the librational mode of methyl groups, as it disappears on deuteration of the methyl group. The peak position of the librational mode of the deuterated methyl group in PI-d_3 should shift via the isotope effect to ca. 17 meV. Its relative scattering intensity decreases strongly for PI-d_3, and thus it is hidden under the broad hump of the backbone librational modes.

The energy of the librational mode position can be related to the energy difference between the librational ground state and the height of the potential well in which the methyl group protons move. The observed value of 23.5 meV is close to values observed for α-methyl protons in poly(methyl methacrylate) (PMMA, 22.5 meV),[1,2] poly(propylene oxide) (PPO, 28.5 meV),[1,2] and polypropylene (PP, 28.7 meV)[4], but much lower than what we have found recently for the sterically hindered polyisobutylene (~40 meV),[13] The width of the observed librational modes, i.e., the distribution of activation energies, and to a minor degree its position are influenced by the local heterogeneity. Thus the methyl group dynamics not only is determined by the microstructure of the polymer but it is also influenced by the surrounding potentials; i.e., interchain effects play an important role. This is very clearly seen in a low molecular weight sample, ethylbenzene, where the width and the position of the methyl group libration are very much affected by either a crystalline or an amorphous environment.[14] Thus the methyl group rotation might be regarded as a probe of the local heterogeneity in polymer glasses. We propose that there is a much narrower distribution of local environments present in PDMS, where the decrease of the elastic scattering is much sharper[5] than in polyisoprene. Polyisobutylene, on the other hand, shows a very broad distribution as evidenced by the broad librational peak and the absence of any methyl group relaxation step for the elastic scattering below the glass transition when measured with an energy resolution of 1 μeV.[16]

The same set of TOF experiments carried out on PI-d_3 and PI-d_5 between 120 and 300 K and with an energy resolution of ca. 80 μeV (fwhm) indicate additional low-frequency contributions (at $E < 1$ meV) from the methyl group but not a clear quasielastic broadening of the elastic line.[17] Quasielastic contributions (in addition to a flat-background, low-frequency inelastic scattering centered at $\pm$1.5 meV and an elastic component) never exceeded the instrumental energy resolution, and the assigned relative intensity was much too small to be attributed to the motion of all methyl group protons. Again a very broad distribution of rotational correlation times as resulting from the elastic scan data might be consistent with this observation.

Up to here only the temperature range below T_g was discussed. As noted above, we find for all samples a further decrease of the elastic intensity near the calorimetric glass transition temperature. A number of inelastic neutron scattering experiments on different kinds of glass formers have shown that this is due to a fast dynamical process arising close to T_g which creates low-frequency or quasielastic scattering in the energy range 0–2 meV. This behavior was discussed in detail for the backbone polymer polybutadiene[6,7] and was found for PI-h_8[8] and PIB[6] as well. Raising the temperature further will lead to a total loss of the elastic scattering; i.e., the elastic line will broaden, a behavior which is expected if translational motions become relevant. As soon as the motion of the scattering particles is no longer restricted t a confined volume and the relaxation times are shorter than the corresponding instrumental resolution, the elastic line will disappear. This is the temperature range where the α-relaxation, i.e., structural relaxation, becomes relevant, and it was shown previously by the neutron spin–echo technique that the temperature dependence of the observed microscopic relaxation times follows the same Vogel–Fulcher-like behavior as the macroscopically measured shear viscosity[12] and agrees with dielectric measurements of the segmental mode.[18] It also can clearly be seen from Figure 2 that the decrease of the elastic scattering is only weakly dependent on the degree of deuteration, thus confirming the conclusion drawn from polybutadiene that the main-chain dynamics in the nano- to picosecond time regime is affected near T_g.

Conclusion

We have reported on incoherent inelastic neutron scattering investigations from fixed-window scans on partially deuterated polyisoprenes. The data show clearly that two dynamical processes occur.

First, the observed onset of dynamics at low temperatures can clearly be assigned to the dynamics of the methyl group. In contrast to expectation, we could not find the characteristic Q-dependences of the elastic form factor for a 3-fold jump or isotropic methyl group rotation and thus cannot determine exactly the type of its reorientation.

Considerable vibrational amplitudes are present in these polymers, which can explain the absence of a pronounced structure in Q for the elastic form factor. Modeling the observed methyl group dynamics by a simple activation behavior results in a far too steep intensity decrease of the elastic scattering. A distribution of local environments of the methyl groups can explain the observed width and also may explain the loss of structure in Q. Fixing the attempt frequency for methyl group rotation at 23.5 meV, the observed vibrational mode, an activation energy of ca. 1550 K describes correctly the midposition of the intensity drop. Good agreement is achieved when choosing a wide activation energy distribution of 28 ± 4%.

The observed second dynamical process is related to the change of the polymer dynamics near the glass transition. In analogy to polybutadiene and other glass-forming systems, the onset of dynamics close to T_g is related to a fast dynamical process in the meV range. At temperatures $T > T_g + 30$ K the α-relaxation contributes further to the observed loss of elastic intensity.

Acknowledgment. B.F. acknowledges the hospitality and support of the National Institute of Standards and Technology during the preparation of the manuscript.

References and Notes

(1) Higgins, J. S.; Allen, G.; Brier, P. N. *Polymer* **1972**, *13*, 157.
(2) Allen, G.; Wright, C. J.; Higgins, J. S. *Polymer* **1974**, *15*, 319.
(3) Gabrys, B.; Higgins, J. S.; Ma, K. T.; Roots, J. E. *Macromolecules* **1984**, *17*, 560.
(4) Takeuchi, H.; Higgins, J. S.; Hill, A.; Maconnachie, A.; Allen, G.; Stirling, G. C. *Polymer* **1982**, *23*, 499.
(5) Grapengeter, H. H.; Alefeld, B.; Kosfeld, R. *Colloid Polym. Sci.* **1987**, *265*, 226.
(6) Frick, B.; Richter, D.; Petry, W.; Buchenau, U. *Z. Phys. B* **1988**, *70*, 73.
(7) Frick, B. *Prog. Colloid Polym. Sci.* **1989**, *80*, 164.
(8) Frick, B.; Richter, D.; Fetters, L. In *Basic Features of the Glassy State*; Colmenero, J., Alegria, A., Eds.; World Scientific: Singapore, 1990; p 204.
(9) Bée, M. In *Quasielastic Neutron Scattering*; Adam Hilger: Bristol, 1988. Barnes, J. D. *J. Chem. Phys.* **1973**, *58*, 5193.
(10) Birr, M.; Alefeld, B.; Heidemann, A. *Nucl. Instrum. Methods* **1971**, *95*, 435.
(11) Lindeman, A. F. *Physik Z.* **1910**, *11*, 609.
(12) Zorn, R.; Richter, D.; Farago, B.; Frick, B.; Kremer, F.; Kirst, U.; Fetters, L. J. *Physica B* **1992**, *180&181*.
(13) Denault, J.; Prud'homme, J. *Macromolecules* **1989**, *22*, 1307.
(14) Frick, B.; Richter, D.; Trevino, S. *Physica A*, to be published.
(15) Frick, B.; Trevino, S.; Williams, J., to be published.
(16) Frick, B.; Richter, D. *Phys. Rev. B* **1993**, *47*, 14795.
(17) Frick, B.; Zorn, R.; Richter, D., to be published.
(18) Kremer, F.; Boese, D.; Meier, G.; Fischer, E. W. *Prog. Colloid Polym. Sci.* **1989**, *80*, 29.
(19) Sears, V. F. In *Thermal Neutron Scattering Lengths and Cross Sections for Condensed Matter Research*, AECL-8490, 1984.